# DMRS-Driven Deep Learning Network for Doppler Estimation in 5G NR-NTN

Ipsita Sannigrahi, Sathish Nallamolu, Pradeep Goutam, Naru Pradeep
Centre for Development of Telematics, Bangalore, India.
{ipsita, sathishn, pradeepg, pradeepn}@cdot.in

***Abstract*—Non-Terrestrial Networks (NTN) in 5G NR experience large Doppler shifts—often reaching tens of kilohertz due to the high relative velocity between satellites and user equipment (UE), particularly in Low Earth Orbit (LEO) systems. Although 3GPP Release-17 introduces Doppler pre-compensation techniques to mitigate this effect, considerable residual frequency errors may persist at the receiver, degrading the coherence of Demodulation Reference Signals (DMRS) and reducing channel estimation accuracy, ultimately affecting communication link performance. This paper proposes a two-stage Doppler estimation that combines DMRS-aware matched-filter spectral learning for coarse acquisition with a deep-learning (DL)-based fine estimator that achieves very low residual errors under realistic SNR conditions. This architecture uses standard NR DMRS symbols, eliminating the need for pilot redesign and maintaining full compatibility with existing NTN PHY processing chains. Simulation results show robust $\pm$40kHz Doppler estimation with errors typically below 200Hz at low computational complexity, enabling practical UE deployments.**

***Index Terms*—5G, NR-NTN, Doppler estimation, DMRS, Deep learning, LEO satellite, Frequency synchronization.**

## I. Introduction

The integration of satellite communication into the 5G New Radio (NR) ecosystem has enabled global connectivity through Non-Terrestrial Networks (NTN), extending coverage to remote, maritime, aeronautical, and other underserved regions [1]. In particular, satellite systems operating in Low Earth Orbit (LEO) have emerged as a key enabler for NTN due to their lower propagation delay and improved link budget compared to Geostationary Earth Orbit (GEO) systems. However, the high orbital velocity of LEO satellites ($\sim$ 7 km/s) introduces severe Doppler shifts that can reach tens of kilohertz at sub-6 $GHz$ carrier frequencies [2]. These large and rapidly varying Doppler effects produce significant carrier frequency offsets that degrade synchronization accuracy, reduce the coherence of demodulation reference signals (DMRS), and negatively impact channel estimation and demodulation performance in NR waveforms.

Unlike terrestrial NR systems, where Doppler shifts are typically limited to a few hundred Hertz, NTN links must contend with Doppler components that are significantly larger and more dynamic in nature. These include Doppler induced by satellite motion, additional Doppler contributions from User Equipment (UE) mobility, such as vehicular or maritime movement, and frequency offsets caused by local oscillator impairments and satellite ephemeris estimation errors [3]. To address these challenges, 3GPP introduced NTN enhancements in Release-17, including Doppler pre-compensation mechanisms based on satellite ephemeris and UE location information. Although gNB-based Doppler pre-compensation significantly reduces the Doppler shift, large uncertainties may still occur during acquisition or when position information is unavailable. The composite Doppler consists of satellite-induced and UE-induced components. The UE-induced Doppler component also requires accurate estimation and fine synchronization, even after gNB Doppler pre-compensation, as per Release-17 for reliability and performance [4].

Conventional Doppler estimation techniques, such as FFT-based maximum-likelihood search, matched filtering, and phase-locked loops, have limitations in NTN environments. Their reliance on long observation windows and stationarity assumptions make them poorly suited for rapidly varying Doppler conditions. Long observation windows also increase computational complexity. Furthermore, achieving fine search resolution across uncertainty ranges spanning tens of kilohertz results in additional computational complexity [5]. Moreover, such methods struggle to jointly accommodate satellite dynamics and UE mobility while preserving compatibility with standardized NR DMRS structures.

Deep learning (DL) is increasingly used to replace or augment classical synchronization and estimation blocks in communication receivers. Learning-based methods applied to pilot signals have demonstrated strong performance in OFDM systems under challenging channel and frequency offset conditions [6]. In 5G NR systems, deep neural networks have also been employed for pilot-assisted channel estimation, demonstrating improved robustness to delay and Doppler variations while maintaining flexibility across deployment scenarios [7]. Building upon these advances, this work proposes a two-stage Doppler estimator for NR-NTN. Stage-1 performs coarse Doppler acquisition using DMRS correlation spectra and a neural classifier over a large Doppler range, while Stage-2 refines the estimate using CNN-based regression on compensated DMRS correlations, enabling sub-200 $Hz$ accuracy

with UE mobility and residual satellite prediction errors. This hybrid approach bridges the performance gap between classical synchronization algorithms and pure deep learning receivers, leveraging the strengths of both to address the unique Doppler characteristics of 5G NR-NTN links.

The remainder of this paper is structured as follows. Section II details the system model and receiver architecture. Section III presents the neural network architecture of both stages. Section IV demonstrates the results and the computational complexity involved. Finally, Section V concludes with the insights gained and outlines the directions for future research.

## II. System Model and Receiver Architecture

### A. NTN Link Geometry and Doppler Components

A forward downlink NR-NTN communication link between a LEO satellite and a terrestrial UE is considered. The relative motion induces a composite Doppler shift that consists of three components:

$$f_d(t) = f_d^{\text{sat}}(t) + f_d^{\text{UE}}(t) + f_d^{\text{osc}}(t), \tag{1}$$

where $f_d^{\text{sat}}(t)$ is the Doppler due to satellite orbital motion, $f_d^{\text{UE}}(t)$ is the Doppler induced by UE mobility, and $f_d^{\text{osc}}(t)$ represents residual frequency offsets from oscillator drift or imperfect ephemeris-based compensation [8]. At a carrier frequency $f_{carrier}$, the Doppler due to the relative radial velocity $v(t)$, where $c$ is the speed of light, is

$$f_d(t) = \frac{v(t)}{c} f_{carrier}. \tag{2}$$

For LEO satellites with a radial velocity of 6 $km/s$ at a carrier frequency of 2 $GHz$, $|f_d^{\text{sat}}|$ may reach $\pm 40$ $kHz$, while UE motion contributes up to several hundred Hertz. Although small compared to satellite Doppler, $f_d^{\text{UE}}$ becomes dominant after coarse compensation and directly impacts fine synchronization accuracy.

### B. NR DMRS-Based Pilot Structure

Doppler estimation relies on the 3GPP NR DMRS as defined in TS 38.211 [9]. The DMRS sequence is generated from the Gold sequence given below.

$$c(n) = (x_1(n + N_c) + x_2(n + N_c)) \pmod 2. \tag{3}$$

The reference symbol is calculated as

$$r[n] = \frac{1}{\sqrt{2}} \left((1 - 2c_{2n}) + j(1 - 2c_{2n+1})\right), \tag{4}$$

where $n = 0, 1, ...., N-1$, and $c(n)$ denotes the Gold sequence initialized by cell-specific parameters. For a 5 $MHz$ bandwidth containing 25 Physical Resource Blocks (PRBs) (300 subcarriers), and assuming three DMRS OFDM symbols per slot, the total number of pilot resource elements used for Doppler estimation is approximately $N = 900$ [10].

### C. Received Baseband Signal Model

The received baseband signal at the UE can be written as:

$$y[n] = h[n]r[n]e^{j2\pi f_d \frac{n}{F_s}} + w[n], \tag{5}$$

where:

- $F_s$ is the sampling frequency. Doppler frequency $f_d \in [-40\,kHz, +40\,kHz]$ represents the composite Doppler. Although the Doppler is inherently time-varying, i.e., $f_d(t)$, as described in Section II-A, it can be approximated as constant over the short DMRS observation interval, leading to $f_d(t) \approx f_d$ within a single estimation window. This assumption is justified by the short duration of DMRS symbols relative to LEO satellite dynamics and is commonly adopted in synchronization and estimation literature.
- $w[n] \sim \mathcal{CN}(0, \sigma^2)$ is complex Gaussian noise (AWGN channel noise).
- $h[n]$ is the channel response. A flat fading AWGN channel is considered over the DMRS, thus $h[n] = h$ and the received signal can be expressed as: $y[n] = hr[n]e^{j2\pi f_d \frac{n}{F_s}} + w[n]$. The proposed method can also be extended to frequency-selective fading scenarios.

### D. Two-Stage Doppler Receiver Architecture

The proposed receiver consists of a coarse Doppler estimator followed by a pure deep-learning fine estimator.

*1) **Stage-1 DL-Driven Coarse Doppler Estimation**:* Unlike conventional ML-based estimators that rely on peak detection over a dense Doppler grid, the proposed approach formulates coarse estimation as a classification problem, eliminating the need for explicit search. The received signal is first correlated with the known DMRS to produce a Doppler frequency spectrum [11]

$$S(f_k) = |\sum_{n=0}^{N-1} y[n]r^*[n]e^{-j2\pi f_k n/F_s}|, \tag{6}$$

where $f_k = [f_{min} + k\Delta f]$, $f_{min}$ = $-40$ $kHz$, $\Delta f = 1$ $kHz$, and $k$ ranges from 0 to 79, yielding uniformly partitioned 80 disjoint bins. Rather than performing a peak search, the normalized spectral vector is input to a neural classifier: $\hat{k} = \arg\max_k p(k \mid S)$, yielding the coarse estimate $\hat{f}_c = f_{min} + (k + \frac{1}{2})\Delta f$.

It is assumed that coarse timing synchronization has already been achieved using standard NR synchronization signals, which ensures time alignment between the received DMRS samples and the locally generated reference sequence. This stage reduces Doppler uncertainty from $\pm 40$ $kHz$ to a local Doppler bin of width 1 $kHz$, while the fine stage is designed to tolerate residual errors up to $\pm 2$ $kHz$ to ensure robustness under coarse-bin misclassification.

*2) **Stage-2 DL-Driven Fine Doppler Estimation**:* After coarse correction:

$$\tilde{y}[n] = y[n]e^{-j2\pi \hat{f}_c \frac{n}{F_s}}$$

Since $z[n] = h\, e^{j2\pi f_r n/F_s} + w''[n]$, the sequence is normalized to remove channel amplitude:

$$\bar{z}[n] = \frac{z[n]}{\sqrt{\frac{1}{N}\sum_n |z[n]|^2}}.$$

This normalized residual-correlated sequence is decomposed into real and imaginary components and fed into a 1-D CNN. The CNN learns to regress $\hat{\boldsymbol{f}}_{\boldsymbol{r}} \in [-\mathbf{2}\boldsymbol{kHz}, +\mathbf{2}\boldsymbol{kHz}]$ with a $\mathbf{tanh}$ activation enforcing bounded outputs. Thus, the final estimated Doppler is: $\hat{\boldsymbol{f}}_{\boldsymbol{d}} = \hat{\boldsymbol{f}}_{\boldsymbol{c}} + \hat{\boldsymbol{f}}_{\boldsymbol{r}}$. A sigmoid-based confidence metric $\mathcal{C} \in [0, 1]$ is also output, providing a reliability metric for decision support.

## III. Neural Network Architectures for Two-Stage Doppler Estimation

This section describes the architectural design of the two neural networks employed in the proposed Doppler estimation framework. In the considered transparent NR-NTN architecture, the satellite operates as a bent-pipe relay. The proposed Doppler estimator is hence implemented at the receiver side of the communication link. In this work, the system model focuses on the UE downlink receiver, while the same architecture can be equivalently applied at the gNB receiver for uplink Doppler estimation.

### *A. Coarse Doppler Classification Model*

The Stage-1 neural network is designed as a multi-class classifier that maps a Doppler-dependent feature vector to a discrete Doppler class. The objective of this model is Doppler localization over a wide frequency range, rather than high-resolution estimation.

- **Input dimension:** $K = 80$ real-valued features corresponding to Doppler bins spanning $\pm 40$ $kHz$ with 1 $kHz$ spacing.
- **Output dimension:** $K = 80$ classes, each representing a Doppler frequency bin.

The output is a probability distribution over Doppler classes. The Stage-1 model follows a fully connected feed-forward architecture as shown in Table I.

TABLE I
Stage-1 Classifier Architecture

| Layer | Neurons / Units | Activation / Details |
|---|---|---|
| Input | 80 (NUM_BINS) | – |
| Dense-1 | 256 | PReLU |
| Dense-2 | 128 | PReLU |
| Output | 80 (NUM_BINS) | Softmax |

The network uses the Adam optimizer for updating the weights. The softmax layer produces normalized posterior probabilities: $p_k = \frac{e^{a_k}}{\sum_{i=1}^{K} e^{a_i}}$, where $a_k$ denotes the pre-activation of class $k$.
Categorical Cross-Entropy is used as the loss function, i.e., $\mathcal{L}_{\text{coarse}} = -\sum_{k=1}^{K} y_k^{smooth} \log(p_k)$ where, $y_k^{smooth}$ and $p_k$ denote the smoothed target and predicted class probabilities, respectively. Label smoothing assigns a small probability to non-target bins, reducing overconfidence and improving robustness near Doppler bin boundaries.

### *B. Fine Doppler Regression Model*

The Stage-2 neural network is designed as a regression model that estimates continuous residual Doppler within a bounded range. Unlike Stage-1, this model operates on time-domain complex samples and targets high-resolution estimation. The input $X$ to this network is a two-channel temporal sequence of length $N = 900$.

$$X = [\Re\{\bar{z}[n]\}, \Im\{\bar{z}[n]\}], n = 0, \ldots, N-1.$$

This representation preserves instantaneous phase evolution, which is directly related to residual Doppler. The Stage-2 model employs a 1-D convolutional neural network (CNN), illustrated in Table II, with the following structure:

TABLE II
Fine-Stage Regression Network Architecture

| Layer | Type | Kernel/Units | Activation |
|---|---|---|---|
| Input | Input | (N_DMRS, 2) | – |
| Block 1 | Conv1D | 32, $K:7$, $S:2$ | PReLU |
| Block 2 | Conv1D | 64, $K:7$ | PReLU |
| | MaxPool1D | Pool: 2 | – |
| Block 3 | Conv1D | 128, $K:5$ | PReLU |
| Pooling | GlobAvgPool1D | – | – |
| Dense | Dense | 64 | PReLU |
| Output 1 | Freq. Out | 1 | Tanh |
| Output 2 | Conf. Out | 1 | Sigmoid |

The network contains two parallel output heads:

- **Residual Doppler head:** $\hat{f}_r = f_{max} tanh(.)$ ensuring bounded regression within $\pm 2$ $kHz$.
- **Confidence head:** The confidence score reflects the consistency of the estimated Doppler with learned DMRS correlation features. To enable the receiver to assess the quality of its own estimates, we incorporate a confidence head. During training, we define a successful estimation as one where the residual error $|\hat{f}_d - f_d| < \epsilon$, where $\epsilon = 200$ $Hz$ is the target precision for NR-NTN synchronization. The binary cross-entropy loss then penalizes the network if it provides a high confidence score for an estimate that exceeds this physical tolerance.

Mean Squared Error is used as the loss function for regression. $\mathcal{L}_{\text{MSE}} = \frac{1}{N}\sum_{i=1}^{N}(\hat{f}_i - f_i)^2$, measures

the squared error between predicted and true residual Doppler. For Confidence score, Binary Cross Entropy is used as loss function. $\mathcal{L}_{\text{BCE}} = -[y_i \log(\hat{y}_i) + (1 - y_i) \log(1 - \hat{y}_i)]$, measures the error in the confidence prediction and encourages reliable uncertainty estimation. Larger kernels in early layers capture coarse Doppler trends, while smaller kernels in deeper layers refine local phase variations, resulting in a multi-resolution representation of Doppler dynamics. The coarse estimator is trained via categorical cross-entropy with label smoothing, while the fine stage utilizes a weighted multi-task objective to jointly optimize for Doppler regression and reliability scoring.

### C. Dataset Generation and Training

Training datasets are generated via Monte Carlo simulations of NR DMRS signals under Doppler and AWGN impairments.A total of $200k$ samples are generated and used for training, with batch sizes of 1024 and 256 for Stage-1 and Stage-2, respectively. Following section II-C, Doppler frequencies are distributed within $\pm 40$ $kHz$, and SNR is randomly selected from $-20$ $dB$ to 10 $dB$ to ensure robustness in low-SNR NTN conditions. This standardized process ensures reproducibility without proprietary data.

## IV. Results

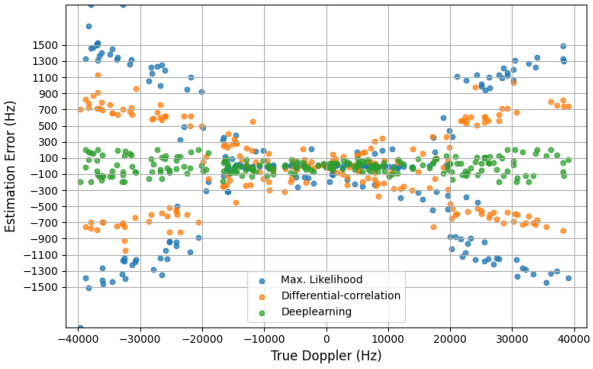


Fig. 1. Performance Comparison of Traditional vs DL

### A. DL vs. Conventional

Unlike traditional correlation-based methods, which struggle with low SNR or phase noise in NTN environments, the proposed estimator exhibits more stable residual error across the evaluated SNR range. For comparison, a classical Maximum Likelihood (ML)-based Doppler estimator is implemented by selecting the frequency bin that maximizes the correlation metric in eq. (6) i.e. $\hat{f}_d = \arg\max_{f_k} S(f_k)$. A differential correlation-based estimation is also performed. Fig. 1 compares the Doppler estimation errors of the proposed DL-based estimator, the ML-based correlation (peak search) estimator, and the differential correlation method across the $\pm 40$ $kHz$ Doppler range, showing lower and more stable errors for the DL-based approach. Classical estimators exhibit higher error variance near Doppler boundaries than the DL-based method.

Fig. 2 shows the RMSE performance of the proposed DL-based Doppler estimator across Doppler and SNR, demonstrating robust and consistent accuracy compared to classical methods. The proposed DL-based estimator therefore offers robustness at low SNR and large Doppler uncertainties. This model can be scaled to wider bandwidths, where the number of PRBs increases to 52 for 10 $MHz$ and 106 for 20 $MHz$, yielding $N = 1872$ and $N = 3816$ DMRS samples, respectively, for 15 $kHz$ subcarrier spacing. The proposed approach can similarly be extended to other numerologies.

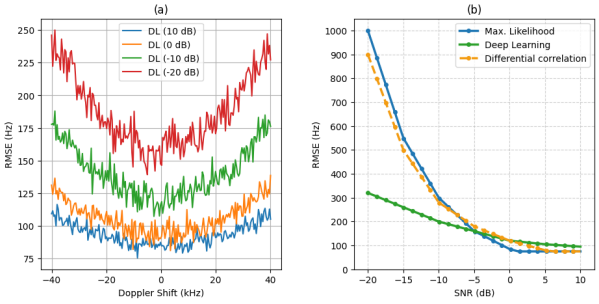


Fig. 2. RMSE vs SNR

### B. Computational Complexity Analysis

Tables III and IV summarize the Floating Operations (FLOPs) count for both models.

TABLE III
FLOPs Calculation for coarse_nn ($N_{BINS} = 80$)

| Layer | Shape In → Out | MAC Formula | Total MACs | Total FLOPs |
|---|---|---|---|---|
| Dense 1 | $80 \to 256$ | $80 \times 256$ | 20,480 | 40,960 |
| PReLU 1 | $256 \to 256$ | Element-wise | 256 | 512 |
| Dense 2 | $256 \to 128$ | $256 \times 128$ | 32,768 | 65,536 |
| PReLU 2 | $128 \to 128$ | Element-wise | 128 | 256 |
| Output | $128 \to 80$ | $128 \times 80$ | 10,240 | 20,480 |
| Softmax | $80 \to 80$ | $\approx 3 \times 80$ | 240 | 480 |
| **Total** | | | **64,112** | **128,224** |

TABLE IV
FLOPs Calculation for fine_nn ($N_{DMRS} = 900$)

| Layer | Output Shape | MAC Calculation | Total MACs | Total FLOPs |
|---|---|---|---|---|
| Conv1D (32) | (450, 32) | $450 \times (7 \times 2 \times 32)$ | 201,600 | 403,200 |
| PReLU 1 | (450, 32) | $450 \times 32$ | 14,400 | 28,800 |
| Conv1D (64) | (450, 64) | $450 \times (7 \times 32 \times 64)$ | 6,451,200 | 12,902,400 |
| PReLU 2 | (450, 64) | $450 \times 64$ | 28,800 | 57,600 |
| MaxPooling | (225, 64) | $225 \times 64$ | 14,400 | 28,800 |
| Conv1D (128) | (225, 128) | $225 \times (5 \times 64 \times 128)$ | 9,216,000 | 18,432,000 |
| PReLU 3 | (225, 128) | $225 \times 128$ | 28,800 | 57,600 |
| GlobAvgPool | (128) | $225 \times 128$ | 28,800 | 28,800 |
| Dense (64) | (64) | $128 \times 64$ | 8,192 | 16,384 |
| PReLU 4 | (64) | 64 | 64 | 128 |
| Outputs (2) | (2) | $64 \times 2$ | 128 | 256 |
| **Total** | | | 15,992,384 | 31,955,968 |

To provide insight into the computational behavior summarized in Table V, the complexity of DL-based

TABLE V
COMPUTATIONAL COMPLEXITY PER NR SLOT

| **Method** | **FLOPs/Slot** | **TOPS** |
|---|---|---|
| DL Stage-1 (Coarse Classifier) | $0.13M$ | 0.00013 |
| DL Stage-2 (Fine Regressor) | $31.96M$ | 0.03196 |
| Proposed DL (Total) | $32.09M$ | 0.03209 |

Doppler estimation is expressed in terms of Trillion Operations per Second (TOPS).

*1) Conventional Doppler Estimation:* Classical Doppler estimators typically perform correlation or FFT-based searches over a Doppler uncertainty range discretized into $B$ frequency bins. For a DMRS sequence of length $N$, the computational complexity can be expressed as

$$\mathcal{C}_{\text{conv}} = \mathcal{O}(N \cdot B),$$

indicating linear growth with Doppler search range and resolution. While hierarchical or binary-search strategies can reduce the number of evaluated frequency hypotheses to approximately $\mathcal{O}(N.logB)$, they still require repeated correlation computations and a sophisticated unimodal search space. The proposed AI-based fine estimator avoids iterative searches altogether by directly regressing the residual Doppler from DMRS observations.

*2) Proposed DL-Based Doppler Estimation:* The proposed two-stage DL-based receiver replaces exhaustive frequency search with fixed-size neural inference. The complexity of Stage-1 coarse Doppler classification is primarily determined by the number of neural network parameters

$$\mathcal{C}_{\text{Stage-1}} = \mathcal{O}\left(\sum_{\ell} N_{\ell-1} N_{\ell}\right),$$

where $N_\ell$ denotes the number of neurons in layer $\ell$. The complexity of Stage-2 fine Doppler regression using a 1-D CNN is given by

$$\mathcal{C}_{\text{Stage-2}} = \mathcal{O}\left(\sum_{m} L_m K_m C_m^{\text{in}} C_m^{\text{out}}\right),$$

where $L_m$, $K_m$, $C_m^{\text{in}}$, and $C_m^{\text{out}}$ represent the output length, kernel size, and input/output channels of the $m$-th convolutional layer, respectively. The total DL inference complexity is independent of Doppler search range. Unlike conventional estimators whose complexity scales linearly with the Doppler search range, the proposed DL-based approach achieves constant-time inference, enabling scalable, hardware-efficient Doppler estimation for high-dynamic NR-NTN systems. This requirement is well within the capabilities of modern UE-grade NPUs, even under fixed-point (INT8) inference. The models are trained offline on an NVIDIA GeForce RTX 4060 GPU for accelerated optimization. Inference is lightweight and can be efficiently executed on mobile processors and UE-grade NPUs.

## V. CONCLUSION AND FUTURE WORK

Simulation results demonstrate that the proposed two-stage estimator typically achieves sub-200 $Hz$ Doppler estimation accuracy under low-SNR NTN conditions while maintaining low computational complexity suitable for UE deployment. To further evolve this AI receiver for 5G-Advanced and 6G standards, future research will focus on several critical enhancements. First, the aim is to implement hardware-aware quantization and model pruning to ensure real-time inference on power-constrained UE without compromising accuracy. Beyond frequency offset, the architecture will be expanded to incorporate Phase Tracking Reference Signals (PTRS) to mitigate Common Phase Error (CPE) and phase noise inherent in high-frequency satellite links. Recurrent Neural Networks (RNNs) or Transformer-based architectures can be used to track the Doppler rate over time, enabling the receiver to maintain synchronization during high-velocity LEO satellite flyovers. Finally, the framework will be adapted for multi-antenna (MIMO) scenarios, utilizing spatial diversity to improve estimation robustness in multi-link NTN environments under challenging interference conditions.

## REFERENCES


[1] 3GPP, "Study on New Radio (NR) to support non-terrestrial networks," 3rd Generation Partnership Project (3GPP), Technical Report (TR) 38.811, 2020.

[2] F. Rossato et al., "5g nr non-terrestrial networks: Open challenges for full-stack protocol design," *arXiv preprint arXiv:2601.14883*, 2026.

[3] M. Hui et al., "A review of leo satellite communication payloads for integrated communication, navigation, and remote sensing: Opportunities, challenges, future directions," *IEEE Internet of Things Journal*, 2025.

[4] X. Tong, Z. Xie, and Y. Gu, "A review of non-terrestrial network standard development in 3gpp ran and future directions for 6g," in *AIAA SciTech 2025 Forum*, 2025, p. 2717.

[5] D. Tian, Y. Zhao, J. Tong, G. Cui, and W. Wang, "Frequency offset estimation for 5g based leo satellite communication systems," in *2019 IEEE/CIC International Conference on Communications in China (ICCC)*, IEEE, 2019, pp. 647–652.

[6] M. Honkala, D. Korpi, and J. M. Huttunen, "Deeprx: Fully convolutional deep learning receiver," *IEEE Transactions on Wireless Communications*, vol. 20, no. 6, pp. 3925–3940, 2021.

[7] P. Saikrishna, A. K. R. Chavva, M. Beniwal, and A. Goyal, "Deep learning based channel estimation with flexible delay and doppler networks for 5g nr," in *2021 IEEE Wireless Communications and Networking Conference (WCNC)*, 2021, pp. 1–6. DOI: 10.1109/WCNC49053.2021.9417313.

[8] A. K. Meshram, S. Kumar, J. Querol, S. Andrenacci, and S. Chatzinotas, "Reduced complexity initial synchronization for 5g nr multibeam leo-based non-terrestrial networks," *IEEE Open Journal of the Communications Society*, 2025.

[9] 3GPP, "NR; Physical channels and modulation," 3rd Generation Partnership Project (3GPP), Technical Specification (TS) 38.211, version v17.0.0, 2022.

[10] I. Tomić, D. Drajić, P. Ivaniš, U. Savković, D. Tešić, and A. Lorić, "Optimized dm-rs configuration for improved 5g new radio network capacity and performance," *Electronics*, vol. 13, no. 11, p. 2028, 2024.

[11] W. Stock, C. A. Hofmann, and A. Knopp, "Correlation-based doppler shift estimation for opportunistic leo-pnt with starlink signals," in *2024 IEEE International Conference on Wireless for Space and Extreme Environments (WiSEE)*, 2024, pp. 130–135. DOI: 10.1109/WiSEE61249.2024.10850255.